

Resonance Raman Spectroscopy and Quantum-Chemical Calculations of Push–Pull Molecules: 4-Hydroxy-4'-nitroazobenzene and Its Anion

Rômulo A. Ando,[†] José L. Rodríguez-Redondo,[‡] A. Sastre-Santos,[‡]
Fernando Fernández-Lázaro,[‡] Gianluca C. Azzellini,[†] Antonio C. Borin,[†] and Paulo S. Santos^{*,†}

Instituto de Química and Instituto do Milênio de Materiais Complexos II, Universidade de São Paulo, Av Lineu Prestes 748, São Paulo SP 05508-000, Brazil, and División de Química Orgánica, Instituto de Bioingeniería, Universidad Miguel Hernández, Avda. del Ferrocarril s/n, Elche 03202, Spain

Received: September 1, 2007; In Final Form: October 18, 2007

The deprotonation of the push–pull molecule 4-hydroxy-4'-nitroazobenzene leads to a substantial variation in the charge distribution over the donor and acceptor moieties in the D- π -azo- π -A system. The extra charge stabilizes the excited state, leading to a drastic red shift of ca. 100 nm in the λ_{\max} of the electronic transition and consequently causes significant changes in the resonance Raman enhancement profiles. In the neutral species the chromophore involves several modes, as $\nu(\text{CN})$, $\nu(\text{NN})$, and $\nu_s(\text{NO}_2)$, while in the anion the selective enhancement of the $\nu_s(\text{NO}_2)$ and $\nu(\text{CO}^-)$ modes indicates a greater geometric variation of the NO_2 and CO^- moieties in the resonant excited electronic state. The interpretation of the electronic transitions and the vibrational assignment are supported by quantum-mechanical calculations, allowing a consistent analysis of the enhancement patterns observed in the resonance Raman spectra.

1. Introduction

Over the last two decades there has been an increasing interest in the theoretical and experimental investigation of push–pull molecules, as is the case of substituted azobenzene derivatives.^{1–6} The main reason for such interest derives from their potential nonlinear optical properties, which in turn depend on appreciable values of the first- or higher-order hyperpolarizabilities (β, γ).^{7–12} Particularly, the first-order hyperpolarizability, β , is related to frequency doubling, and it is now well-known that appreciable values of β are achieved in noncentrosymmetric structures bearing a highly delocalized π framework to which electron-withdrawing and electron-donating groups are attached in suitable positions.^{13–16} As a consequence, such species display intense charge-transfer transitions in the visible near UV spectrum that in general present substantial solvatochromic effect.^{17,18} In particular, azobenzene derivatives have been thoroughly investigated with views to a better understanding of their potential isomerization around the azo linkage.^{19–21} This kind of study depends critically on detailed knowledge of the nature of the excited electronic states that are populated during the photoisomerization process. In particular, it is now acknowledged that the presence of push–pull moieties in the azobenzene framework speeds up significantly the isomerization process.²² Moreover, in a recent publication it was shown that the 4-hydroxy-4'-nitroazobenzene anion axially linked to a silicon–phthalocyanine is a rather efficient molecular moiety for the fluorescence quenching modulated by the isomerization state.²³

However, as a consequence of the high asymmetry of the charge distribution in the excited electronic state, it is to be expected that push–pull molecules display a particularly strong enhancement in their Raman spectra, showing the modes directly

involved in the charge-transfer process. In fact, resonance Raman spectroscopy is the technique of choice to monitor the extent of the electronic delocalization in the chromophoric units of such molecules.

In the present work, UV–vis and resonance Raman spectroscopies, together with quantum-mechanical calculations, are employed to investigate the chromophore delocalization in 4-hydroxy-4'-nitroazobenzene as well as in its deprotonated species. In particular, the effect of the extra charge in the anion is assessed, comparing the enhancement pattern in the two species. In addition, to support the interpretation of the experimental results, quantum-chemical calculations were performed using the complete active space self-consistent field and multiconfigurational second-order perturbation (CASSCF/CASPT2) protocol^{24–26} that provides the calculated vertical electronic transitions and the harmonic vibrational frequencies.

2. Experimental Section

4-Hydroxy-4'-nitroazobenzene was prepared in 72% yield, after column chromatography, by a described procedure starting from 4-nitroaniline.²⁷ The latter was reacted with isoamyl nitrite and hydrochloric acid to yield the corresponding diazonium salt, which was coupled with phenol under basic conditions. The compound was characterized by ¹H NMR and UV–vis and IR spectroscopies.

The UV–vis spectra were obtained in methanolic acidic (pH = 5) and basic (pH = 9) solutions (5×10^{-4} M) in a Shimadzu UVPC 3010. The respective Raman spectra, excited by several lines (406.7–647.1 nm) of Ar⁺ and Kr⁺ lasers (Coherent INNOVA 90–6), were obtained in a Jobin-Yvon U1000 double spectrometer, with photomultiplier detection (Hamamatsu, RCA-A02 at –20 °C). The ca. 1038 cm⁻¹ Raman band of CH₃OH was used as an internal standard. The laser beam was focused on the samples with ca. 50–200 mW of laser power, and to avoid local heating the sample was contained in a small NMR tube coupled to a rotator shaft.

* Author to whom correspondence should be addressed. Phone: 55-11-30913853. Fax: 55-11-30913890. E-mail: pssantos@iq.usp.br.

[†] Universidade de São Paulo.

[‡] Universidad Miguel Hernández.

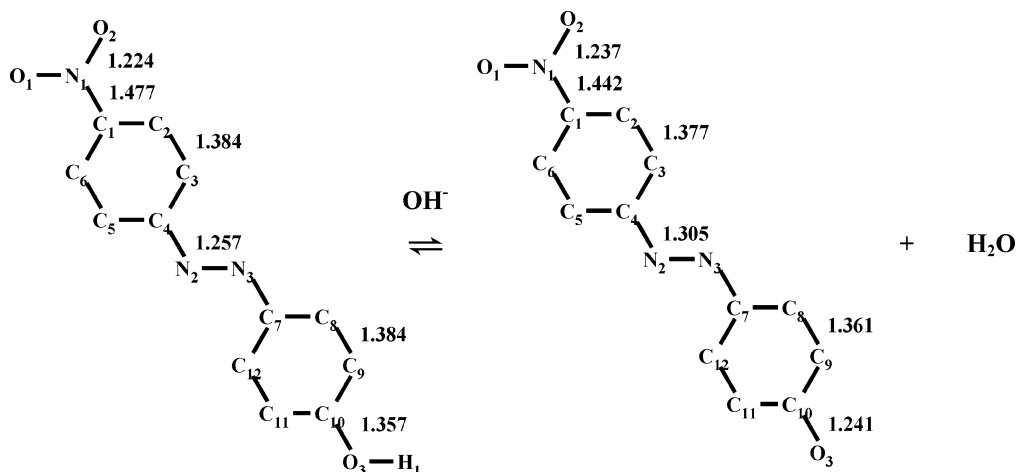


Figure 1. Structures of neutral 4-hydroxy-4'-nitroazobenzene and its anion, with the corresponding atom numbering and some calculated interatomic distances.

TABLE 1: Calculated Bond Lengths and Angles for 4-Hydroxy-4'-nitroazobenzene and Its Anion

	neutral	anion		neutral	anion
Bond Lengths (Å)					
N ₁ -O ₁	1.224	1.237	N ₂ -N ₃	1.257	1.305
N ₁ -O ₂	1.224	1.237	C ₁₀ -O ₃	1.357	1.241
C ₁ -N ₁	1.477	1.442	O ₃ -H ₁	0.963	
N ₂ -C ₄	1.417	1.375	N ₃ -C ₇	1.405	1.346
C ₁ -C ₂	1.395	1.404	C ₇ -C ₈	1.402	1.432
C ₂ -C ₃	1.384	1.377	C ₈ -C ₉	1.384	1.361
C ₃ -C ₄	1.405	1.422	C ₉ -C ₁₀	1.398	1.462
C ₄ -C ₅	1.400	1.418	C ₁₀ -C ₁₁	1.404	1.467
C ₅ -C ₆	1.388	1.378	C ₁₁ -C ₁₂	1.383	1.359
C ₁ -C ₆	1.391	1.402	C ₇ -C ₁₂	1.405	1.437
Bond Angles (deg)					
O ₁ -N ₁ -O ₂	124.76	122.93	C ₄ -N ₂ -N ₃	114.61	113.89
C ₁ -N ₁ -O ₁	117.63	118.52	N ₂ -N ₃ -C ₇	115.71	117.12
C ₁ -N ₁ -O ₂	117.61	118.55	C ₁₀ -O ₃ -H ₁	109.73	
N ₁ -C ₁ -C ₂	118.97	119.86	N ₃ -C ₇ -C ₈	115.98	116.83
N ₁ -C ₁ -C ₆	118.98	119.79	N ₃ -C ₇ -C ₁₂	124.77	125.53
N ₂ -C ₄ -C ₅	115.53	116.56	C ₁₁ -C ₁₀ -O ₃	122.43	122.23
N ₂ -C ₄ -C ₃	124.60	125.80	C ₉ -C ₁₀ -O ₃	117.44	122.83
C ₁ -C ₂ -C ₃	119.04	120.02	C ₇ -C ₈ -C ₉	120.93	121.96
C ₂ -C ₃ -C ₄	119.98	120.94	C ₈ -C ₉ -C ₁₀	119.44	121.83
C ₃ -C ₄ -C ₅	119.87	117.64	C ₉ -C ₁₀ -C ₁₁	120.13	114.94
C ₄ -C ₅ -C ₆	120.54	121.61	C ₁₀ -C ₁₁ -C ₁₂	120.16	122.58
C ₅ -C ₆ -C ₁	118.52	119.44	C ₁₁ -C ₁₂ -C ₇	120.10	121.04
C ₆ -C ₁ -C ₂	122.05	120.35	C ₈ -C ₇ -C ₁₂	119.25	117.64

Theoretical Methods. The ground-state geometry of the 4-hydroxy-4'-nitroazobenzene and its anion were fully optimized employing the density functional theory (DFT) with the B3LYP²⁸⁻³⁰ hybrid functional (Becke's gradient-corrected exchange correlation in conjunction with the Lee-Yang-Parr correlation functional with three parameters) and the 6-311G-(d,p) one-electron atomic basis sets. The nuclear framework was assumed to be of *C_s* symmetry. In a second step, frequency analysis was carried out, and no imaginary frequencies were found, indicating that the optimized geometries were in a minimum of the potential energy surface. Geometry optimizations were performed with the aid of the Gaussian 03 software.³¹

The vertical electronic spectra were computed at the B3LYP-optimized geometries employing the CASSCF/CASPT2 protocol,²⁴⁻²⁶ following a similar approach adopted by us recently,³² with the aid of the MOLCAS 6.4 software.³³ Carbon, nitrogen, and oxygen atoms were described by double- ζ with polarization atomic natural orbital (ANO) basis sets;³⁴ the shifted zero-order Hamiltonian was proposed by Ghigo et al. (shift parameter of

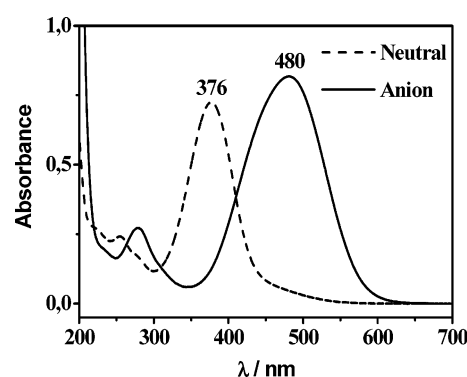


Figure 2. Electronic spectra of 4-hydroxy-4'-nitroazobenzene in acidic and basic methanolic solutions.

TABLE 2: Mulliken Charges for Individual Atoms in 4-Hydroxy-4'-nitroazobenzene and Its Anion in the Ground (*S*₀) and Excited (*S*₁) Electronic States

atom	charge (Mulliken)			
	ground state (<i>S</i> ₀)		excited state (<i>S</i> ₁)	
	neutral	anion	neutral	anion
N ₁	0.2629	0.1962	0.2646	0.1722
N ₂	-0.2700	-0.3987	-0.3350	-0.3056
N ₃	-0.2560	-0.3029	-0.3563	-0.2609
O ₁	-0.3554	-0.3386	-0.3645	-0.4115
O ₂	-0.3539	-0.3352	-0.3638	-0.4111
O ₃	-0.2902	-0.6276	-0.2717	-0.5923
C ₁	0.3642	0.3206	0.3469	0.2831
C ₂	-0.0692	-0.0849	-0.0787	-0.0924
C ₃	-0.1181	-0.1489	-0.1312	-0.1750
C ₄	0.1953	0.2053	0.2020	0.1638
C ₅	-0.0507	-0.0689	-0.0633	-0.0694
C ₆	-0.0681	-0.0861	-0.0798	-0.1115
C ₇	0.1566	0.1013	0.2528	0.1849
C ₈	-0.0365	-0.0002	0.0359	-0.0211
C ₉	-0.1024	-0.1680	-0.1554	-0.1173
C ₁₀	0.3443	0.3790	0.3635	0.3640
C ₁₁	-0.1571	-0.1388	-0.0620	-0.1272
C ₁₂	0.1081	-0.0945	-0.1493	-0.1138
H ₁	0.1871		0.1912	

0.25 hartree).³⁵ Intruder states interacting weakly with the reference functions were removed with an imaginary level shift of 0.1 au.³⁶

After a series of test calculations, the active space employed for computing the excited states of $\pi\pi^*$ character was built, distributing 14 electrons in 13 molecular orbitals, denoted by CASSCF(14,13). Reference functions for the ground and excited

TABLE 3: Experimental and Computed (CASPT2) Vertical Excitation Energies (E), Related Oscillator Strengths (f), and CASSCF Dipole Moments for the Ground and Excited States of 4-Hydroxy-4'-nitroazobenzene and Its Anion

state	neutral				anion			
	$E_{\text{exp}}^a/\text{eV}$	$E_{\text{calc}}^a/\text{eV}$	f	μ (D)	$E_{\text{exp}}^a/\text{eV}$	$E_{\text{calc}}^a/\text{eV}$	f	μ (D)
ground (S_0)				6.22				9.22
1 ¹ A (S_1)	3.30 (376)	3.92 (316)	0.2594	11.22	2.58 (480)	2.25 (551)	1.2815	1.02
2 ¹ A (S_2)		4.08 (304)	0.2859	14.11		3.60 (344)	0.0027	3.16
3 ¹ A (S_3)		4.32 (287)	0.0100	4.88		3.87 (321)	0.0141	2.74

^a Values in parentheses are in nanometers.

TABLE 4: Approximate Description of the Most Relevant Raman Modes (Experimental and Calculated Frequencies) for 4-Hydroxy-4'-nitroazobenzene and Its Anion

neutral			anion		
exp/cm ⁻¹	calc/cm ⁻¹	assignment	exp/cm ⁻¹	calc/cm ⁻¹	assignment
550	550	ϕ	554	554	ϕ
802	806	ϕ	802		$\gamma(\text{CH})$
834	821	$\gamma(\text{CH})$		825	$\phi(1)$
861	877	$\delta(\text{NO}_2) + \phi(1)$	858	863	$\delta(\text{NO}_2) + \phi(1)$
925	942	$\delta(\text{NN}) + \phi(1)$	923	917	$\delta(\text{NN}) + \phi(1)$
1009	1019	$\phi(12)$	1007	1009	$\phi(12)$
	1024	$\delta(\text{CH})$		1094	$\delta(\text{CH})$
1109	1119	$\nu(\text{C}-\text{NO}_2) + \delta(\text{CH})$	1106	1119	$\nu(\text{C}-\text{NO}_2) + \delta(\text{CH}) + \nu_s(\text{NO}_2)$
	1122	$\delta(\text{CH})$	1129	1122	$\delta(\text{CH}) + \nu(\text{C}-\text{NO}_2)$
1140	1158	$\nu(\text{CN})$	1153	1152	$\delta(\text{CH})$
1183	1198	$\delta(\text{OH})$	1190	1182	$\delta(\text{CH})$
1232	1210	$\delta(\text{CH}) + \delta(\text{OH})$	1237	1245	$\nu(\text{NN}) + \delta(\text{CH})$
1248	1265	$\nu(\text{C}-\text{NN})$	1265	1257	$\delta(\text{CO})$
1292	1303	$\delta(\text{CH}) + \nu(\text{CO})$	1294	1290	$\nu_s(\text{NO}_2) + \nu(\text{NN}) + \delta(\text{CH})$
			1327	1307	$\delta(\text{CH})$
1346	1373	$\nu_s(\text{NO}_2) + \nu(\text{CN}) + \delta(\text{OH})$	1342	1347	$\nu_s(\text{NO}_2) + \nu(\text{CN})$
	1379	$\delta(\text{OH})$	1385	1361	$\nu(\text{NN}) + \nu_s(\text{NO}_2) + \delta(\text{CH})$
1407		$\nu(\text{NN})$	1423	1454	$\nu(\text{CN}) + \delta(\text{CH})$
1438	1439	$\nu(\text{NN}) + \delta(\text{CH})$			
1455	1470	$\nu(\text{NN}) + \delta(\text{CH}) + \delta(\text{OH})$	1447	1469	$\nu(\text{CC}) + \delta(\text{CH})$
1505	1501	$\delta(\text{CH}) + \nu(\text{NN})$		1511	$\nu(\text{CN}) + \delta(\text{CH})$
			1508	1531	$\nu_{\text{as}}(\text{NO}_2) + \phi(8\text{a})$
	1544	$\delta(\text{CH}) + \nu(\text{NN})$		1553	$\nu(\text{CC})$
1592	1594	$\phi(8\text{a}) + \nu_{\text{as}}(\text{NO}_2)$	1587	1602	$\phi(8\text{a}) + \nu_{\text{as}}(\text{NO}_2)$
1606	1638	$\phi(8\text{a})$		1626	$\nu(\text{CO}) + \nu(\text{CC})$
1659	1651	$\nu(\text{CO}) + \phi(12)$	1652	1667	$\nu(\text{CO}) + \phi(12)$

1(π, π^*) electronic states were obtained from average CASSCF calculations, including in the averaging the first four lowest-lying 1(π, π^*) electronic states, except for the ground state that was computed with the same active space in a state-specific calculation. Core orbitals were kept frozen in the form determined by the ground-state closed-shell Hartree–Fock wave function, at both CASSCF and CASPT2 steps. Oscillator strengths (f) were computed by combining the transition dipole moments from the ground to the excited states, computed from the CASSCF wave functions obtained as described above with the aid of the CASSCF state interaction method,^{37,38} and the vertical transition energies obtained at the CASPT2 level.

3. Results and Discussion

Figure 1 displays schematically the structures of the investigated species in neutral and anionic forms, with the corresponding atom numbering and the calculated interatomic distances. The calculated (vacuum) values of interatomic distances and angles are shown in Table 1. The variation of the geometric parameters with the deprotonation suggests that, in the case of the anion, a quinoid structure should be considered, even in the ground electronic state,³² because there is a shortening of C₁–N₁, C₂–C₃, C₈–C₉, and C₁₀–O₃ bonds as shown in Figure 1. In addition, there is an increase of the N–O bond lengths, with a concomitant increase in the charge density at the oxygen atoms of the NO₂ moiety with deprotonation. It is also worth mentioning the significant increase in the azo (N=N) bond distance in going from the neutral to the anionic species, as a consequence of the higher electronic delocalization.

In Table 2 are displayed the Mulliken charges for individual atoms in both neutral 4-hydroxy-4'-nitroazobenzene and its anion. The deprotonation of the hydroxy group leads to a substantial redistribution of negative charge to the N₂ atom of the N₁=N₂ moiety and to the O₃ atom of the CO⁻ moiety. In addition, in the anion there is a considerable negative charge at the oxygen atoms of the NO₂ group, thus pointing out the significant effect of the powerful electron acceptor NO₂ group in the stabilization of the anionic structure. Such charge redistribution is in line with the observed red shift of the λ_{max} from the neutral to the anionic species, because both N=N and CO moieties become much better donors in the anionic species.

Figure 2 shows the electronic (UV–vis) spectra of 4-hydroxy-4'-nitroazobenzene and its respective anion in CH₃OH solution. The dramatic red shift ($\Delta\lambda_{\text{max}} \approx 100$ nm) and the increase of the integrated intensity of the low-energy electronic transition with deprotonation are noticeable.

The experimental excitation energies and the values of the calculated vertical transition energies are reported in Table 3, together with the dipole moments for the ground and excited states for the neutral and anionic species. It is worth mentioning that the quantum-chemical calculations were performed in vacuum (gas phase) and the discrepancies with experimental values (solution) are quite acceptable, because push–pull chromophores generally have a pronounced solvatochromic effect. The most relevant molecular orbitals involved in the lowest-energy electronic transitions are plotted in Figure 3.

For the neutral species, the strongest electronic absorption band recorded experimentally in methanolic solutions is located

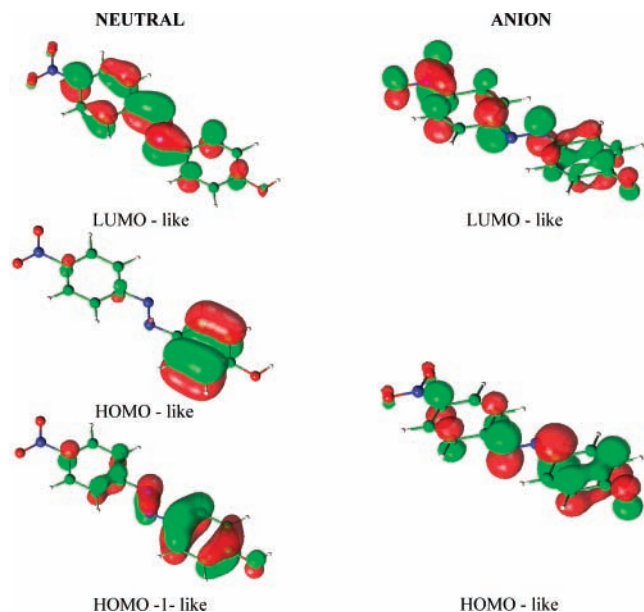


Figure 3. Contours of the molecular orbitals involved in the low-energy electronic transitions for 4-hydroxy-4'-nitroazobenzene and its anion.

at 376 nm, which correlates with the first excited state computed at the 316 nm at CASPT2 level, corresponding to the $S_1 \leftarrow S_0$ ($\pi\pi^*$) electronic transition. On the basis of the population of the natural orbitals (NOs) of the CASSCF wave function, the S_1 excited state is derived from the ground state (S_0) by a two one-electron promotions to the NO equivalent to the lowest-lying unoccupied molecular orbital (LUMO-like), being one from the NO equivalent to the highest occupied molecular orbital (HOMO-like \rightarrow LUMO-like) and the other from the HOMO-1-like molecular orbital (HOMO-1-like \rightarrow LUMO-like). The CASSCF wave function for S_1 is, thus, described by two configurations (weights in parentheses): (HOMO-like \rightarrow LUMO-like) (30%), (HOMO-1-like \rightarrow LUMO-like) (17%). Upon excitation, the dipole moment varies from 6.22 D (S_0 state) to 11.22 D (S_1 state). As can be seen in Figure 3 (natural orbitals), during the vertical transition from the S_0 to the S_1 states the main contribution to the electron reorganization comes from a transfer of electron density from the "phenol-like" moiety to the N_1 - N_2 bond region. This pattern correlates with the variation in the corresponding Mulliken charges, which for the N_1 atom goes from $-0.26e$ (ground state) to $-0.36e$ (excited state) and for the N_2 atom from $-0.27e$ to $-0.33e$, respectively.

A similar discussion can be performed for the anion. Experimentally, the strongest electronic absorption band is located at 480 nm, which correlates nicely with the CASPT2 transition computed at 551 nm; it corresponds to the $S_1 \leftarrow S_0$ ($\pi\pi^*$) electronic transition. In terms of the NO occupation numbers, the S_1 excited state of the anion is obtained by single-electron promotion from the HOMO-like to LUMO-like molecular orbitals, with a CASSCF wave function dominated by the single HOMO-like \rightarrow LUMO-like electronic configuration. The CASSCF S_1 dipole moment is 1.02 D, while the corresponding value for the ground state is 9.22 D. Unlike the neutral species, upon vertical excitation (Figure 3) one observes a transfer of charge density to the NO_2 moiety, especially to its oxygen atoms, which can also be observed by analyzing the changes in the Mulliken charge densities of the corresponding atoms at the ground and excited states (values in parentheses, respectively): N_1 ($+0.20e$, $0.17e$), O_1 ($-0.33e$, $-0.41e$), and O_2 ($-0.34e$, $-0.41e$).

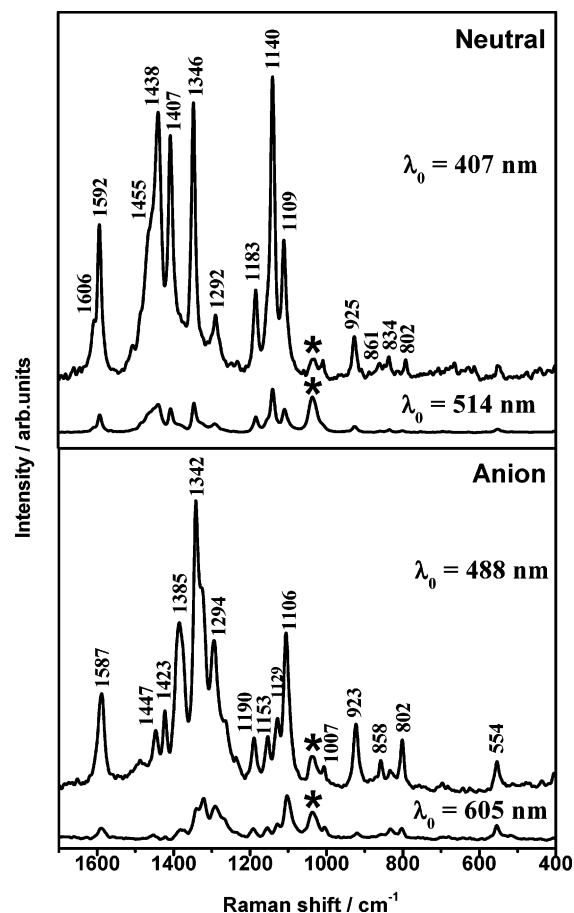


Figure 4. Normal and resonance Raman spectra of neutral and anionic species of 4-hydroxy-4'-nitroazobenzene in methanolic solutions. The asterisks indicate the internal standard at 1038 cm^{-1} (CH_3OH).

Figure 4 shows the normal and resonance Raman spectra of the neutral and anionic species, while Table 4 displays the experimental and calculated Raman frequencies for the more relevant vibrational modes, with the corresponding assignments.

In the resonance Raman spectrum of the neutral species there is a very substantial enhancement of several modes, as the symmetric stretching of the NO_2 mode, $\nu_s(\text{NO}_2)$ at ca. 1346 cm^{-1} , the $\nu(\text{C}-\text{NN})$ at ca. 1140 cm^{-1} , azo group stretching, $\nu(\text{N}=\text{N})$ at ca. 1438 and 1407 cm^{-1} , and ring modes at ca. 1592 and 1183 cm^{-1} , and $\nu(\text{C}-\text{NO}_2)$ at ca. 1109 cm^{-1} . This reveals the great electronic delocalization of the lower-energy electronic transition ($S_0 \rightarrow S_1$) with the participation of several molecular moieties in the chromophoric unit, as observed in CASPT2 calculations.

In the case of the anionic species the resonance Raman spectrum shows that the $\nu_s(\text{NO}_2)$ mode is the most enhanced one at ca. 1342 cm^{-1} , alongside several ring modes at ca. 1587 , 1385 , and 1106 cm^{-1} . The lower enhancement of the modes associated with the azo moiety as $\nu(\text{C}-\text{NN})$ at ca. 1129 cm^{-1} and $\nu(\text{NN})$ at ca. 1447 and 1423 cm^{-1} suggests that the lowest electronic transition ($S_0 \rightarrow S_1$) involves mainly the NO_2 moiety, corroborating the patterns observed in quantum-chemical calculation results.

4. Conclusion

Resonance Raman spectroscopy and quantum-chemical calculations for 4-hydroxy-4'-nitroazobenzene and its anion have shown a considerable charge redistribution in the parent molecule after deprotonation, as indicated by the substantial red

shift of the electronic transition and the change in the extension of the chromophore delocalization revealed by resonance Raman patterns.

Acknowledgment. The authors acknowledge FAPESP (Grant No. 01/09497-8), CNPq, CAPES, Instituto do Milênio de Materiais Complexos II, and the Spanish CICYT (Grant No. MAT2005-07369-C03-02). A.C.B. acknowledges computer time from the Laboratório de Computação Científica Avançada of the Universidade de São Paulo.

References and Notes

- (1) Biswas, N.; Umaphathy, S. *J. Chem. Phys.* **1997**, *107*, 7849.
- (2) Biswas, N.; Umaphathy, S. *J. Raman Spectrosc.* **2001**, *32*, 471.
- (3) Biswak, A. M.; Abraham, B.; Umaphathy, S. *J. Phys. Chem. A* **2002**, *106*, 9397.
- (4) Biswas, N.; Umaphathy, S. *J. Chem. Phys.* **2003**, *118*, 5526.
- (5) Itoh, T.; McCreery, R. L. *J. Am. Chem. Soc.* **2002**, *124*, 10894.
- (6) Nowak, A. M.; McCreery, R. L. *J. Am. Chem. Soc.* **2004**, *126*, 16621.
- (7) Prasad, P. N.; Williams, D. J. *Introduction to Nonlinear Optical Effects in Molecules and Polymers*; John Wiley & Sons: New York, 1991.
- (8) Facchetti, A.; Abbotto, A.; Beverina, L.; van der Boom, M. E.; Dutta, P.; Evmenenko, G.; Marks, T. J.; Pagani, G. A. *Chem. Mater.* **2002**, *14*, 4996.
- (9) Innocenzia, P.; Lebeau, B. *J. Mater. Chem.* **2005**, *15*, 3821.
- (10) Cui, Y.; Qian, G.; Gao, J.; Chen, L.; Wang, Z.; Wang, M. *J. Phys. Chem. B* **2005**, *109*, 23295.
- (11) Tirelli, N.; Suter, U. W.; Altomare, A.; Solaro, R.; Ciardelli, F.; Follonier, S.; Bosshard, C.; Günter, P. *Macromolecules* **1998**, *31*, 2152.
- (12) Antonov, L.; Kamada, K.; Nedeltcheva, D.; Ohta, K.; Kamounah, F. S. *J. Photochem. Photobiol., A* **2006**, *181*, 274.
- (13) Roviello, A.; Sarcinelli, F. *Opt. Mater.* **2005**, *27*, 1800.
- (14) McDonagh, A. M.; Lucas, N. T.; Cifuentes, M. P.; Humphrey, M. G.; Houbrechts, S.; Persoons, A. *J. Organomet. Chem.* **2000**, *605*, 184.
- (15) Jeon, B.; Cha, S.; Jeong, M.; Lim, T. K.; Jin, J. *J. Mater. Chem.* **2002**, *12*, 546.
- (16) Tu, Y.; Luo, Y.; Agren, H. *J. Phys. Chem. B* **2006**, *110*, 8971.
- (17) Matczyszyn, K.; Bartkowiaka, W.; Leszczynski, J. *J. Mol. Struct.* **2001**, *53*, 565.
- (18) Airinei, A.; Rusu, E.; Dorohoi, D. *Spectrosc. Lett.* **2001**, *34*, 65.
- (19) Sokalski, W. A.; Góra, R. W.; Bartkowiak, W.; Kobylinski, P.; Sworakowski, J.; Chyla, A. *J. Chem. Phys.* **2001**, *114*, 5504.
- (20) Fliegl, H.; Kohn, A.; Hattig, C.; Ahlrichs, R. *J. Am. Chem. Soc.* **2003**, *125*, 9821.
- (21) Hagiri, M.; Ichinose, N.; Zhao, C.; Horiuchi, H.; Hiratsuka, H.; Nakayama, T. *Chem. Phys. Lett.* **2004**, *391*, 297.
- (22) Schmidt, B.; Sobotta, C.; Malkmus, S.; Laimgruber, S.; Braun, M.; Zinth, W.; Gilch, P. *J. Phys. Chem. A* **2004**, *108*, 4399.
- (23) Rodríguez-Redondo, J. L.; Sastre-Santos, A.; Fernández-Lázaro, F.; Soares, D.; Azzellini, G. C.; Elliott, B.; Echegoyen, L. *Chem. Commun.* **2006**, *12*, 1265.
- (24) Roos, B. O. In *Ab Initio Methods in Quantum Chemistry II*; Lawley, K. P., Ed.; Advances in Chemical Physics 69; John Wiley & Sons: Chichester, U. K., 1987.
- (25) Andersson, K.; Malmqvist, P. A.; Roos, B. O.; Sadlej, A. J.; Wolinski, K. *J. Phys. Chem.* **1990**, *94*, 5483.
- (26) Andersson, K.; Malmqvist, P. A.; Roos, B. O. *J. Chem. Phys.* **1992**, *96*, 1218.
- (27) Haghbeen, K.; Tan, E. W. *J. Org. Chem.* **1998**, *63*, 4503.
- (28) Becke, A. D. *J. Chem. Phys.* **1993**, *98*, 5648.
- (29) Lee, C.; Yang, W.; Parr, R. G. *Phys. Rev. B* **1988**, *37*, 785.
- (30) Stephens, P. J.; Devlin, F. J.; Chabalowski, C. F.; Frish, M. J. *J. Phys. Chem.* **1994**, *98*, 11623.
- (31) Frisch, M. J.; Trucks, G. W.; Schlegel, H. B.; Scuseria, G. E.; Robb, M. A.; Cheeseman, J. R.; Montgomery, J. A., Jr.; Vreven, T.; Kudin, K. N.; Burant, J. C.; Millam, J. M.; Iyengar, S. S.; Tomasi, J.; Barone, V.; Mennucci, B.; Cossi, M.; Scalmani, G.; Rega, N.; Petersson, G. A.; Nakatsuji, H.; Hada, M.; Ehara, M.; Toyota, K.; Fukuda, R.; Hasegawa, J.; Ishida, M.; Nakajima, T.; Honda, Y.; Kitao, O.; Nakai, H.; Klene, M.; Li, X.; Knox, J. E.; Hratchian, H. P.; Cross, J. B.; Bakken, V.; Adamo, C.; Jaramillo, J.; Gomperts, R.; Stratmann, R. E.; Yazyev, O.; Austin, A. J.; Cammi, R.; Pomelli, C.; Ochterski, J. W.; Ayala, P. Y.; Morokuma, K.; Voth, G. A.; Salvador, P.; Dannenberg, J. J.; Zakrzewski, V. G.; Dapprich, S.; Daniels, A. D.; Strain, M. C.; Farkas, O.; Malick, D. K.; Rabuck, A. D.; Raghavachari, K.; Foresman, J. B.; Ortiz, J. V.; Cui, Q.; Baboul, A. G.; Clifford, S.; Cioslowski, J.; Stefanov, B. B.; Liu, G.; Liashenko, A.; Piskorz, P.; Komaromi, I.; Martin, R. L.; Fox, D. J.; Keith, T.; Al-Laham, M. A.; Peng, C. Y.; Nanayakkara, A.; Challacombe, M.; Gill, P. M. W.; Johnson, B.; Chen, W.; Wong, M. W.; Gonzalez, C.; Pople, J. A. *Gaussian 03*, revision D.01; Gaussian, Inc.: Wallingford, CT, 2004.
- (32) Ando, R.; Borin, A. C.; Santos, P. S. *J. Phys. Chem A* **2007**, *111*, 7194.
- (33) Karlström, G.; Lindh, R.; Malmqvist, P. A.; Roos, B. O.; Ryde, U.; Veryazov, V.; Widmark, P. O.; Cossi, M.; Schimmelpfennig, B.; Neogrady, P.; Seijo, L. *Comput. Mater. Sci.* **2003**, *28*, 222.
- (34) Widmark, P. O.; Malmqvist, P. A.; Roos, B. O. *Theor. Chim. Acta* **1990**, *77*, 291.
- (35) Ghigo, G.; Roos, B. O.; Malmqvist, P. A. *Chem. Phys. Lett.* **2004**, *396*, 142.
- (36) Forsberg, N.; Malmqvist, P. A. *Chem. Phys. Lett.* **1997**, *274*, 196.
- (37) Malmqvist, P. A. *Int. J. Quantum Chem.* **1986**, *30*, 479.
- (38) Malmqvist, P. A.; Roos, B. O. *Chem. Phys. Lett.* **1989**, *155*, 189.